Available online at www.sciencedirect.com
SCIENCE DIRECT®
Chemical Physics Letters 390 (2004) 50–54
CHEMICAL PHYSICS LETTERS
www.elsevier.com/locate/cplett

Photoionization of NO($A^2\Sigma^+$, $v = 0, N$) at 226 nm: ion-recoil momentum spectroscopy

Alexei I. Chichinin [a,b], Tina S. Einfeld [a], Christof Maul [a,*], Karl-Heinz Gericke [a]

[a] Institut für Physikalische und Theoretische Chemie, Technische Universität Braunschweig, Hans-Sommer-Str. 10, 38106 Braunschweig, Germany
[b] Institute of Chemical Kinetics and Combustion, 630090 Novosibirsk, Russia

Received 10 February 2004; in final form 31 March 2004
Available online 27 April 2004

Abstract

We report the first observation of ion recoil induced by the ionization process for a molecule. The applicability of the method has been demonstrated by determining the β_2 and β_4 anisotropy parameters of the angular distributions of NO^+ ions in the resonance-enhanced two-photon ionization of NO($X^2\Pi_{1/2}$, $v = 0, J$) via the $A^2\Sigma^+(v^* = 0, N^*)$ state at 226 nm. An energy resolution in the range of 10 μeV is demonstrated. The method might prove to be particularly useful for studying complex ionization-fragmentation processes as they occur for example for superexcited molecules.

1. Introduction

Recoil-ion momentum spectroscopy has become a useful tool for the study of different ionization and electron exchange processes, including ion–atom collisions [1–8], dissociative photoionization of diatomic molecules [9], ionization of atoms and molecules by strong electric field [10], and resonant multiphoton photoionization of laser-cooled atoms [11,12]. In many cases photoelectron spectroscopy (PES) is also applicable with a better resolution than for ion recoil measurements. In recoil-ion momentum spectroscopy the main problem is the determination of a tiny heavy particle momentum change upon light electron ejection. However, ion recoil spectroscopy allows to study fragmentation and ionization processes for molecules and molecular ions together which cannot be accomplished by photoelectron spectroscopy. The best approach is the application of both techniques to detect recoil ions in coincidence with photoelectrons [5,7].

Here, we present the first application of recoil-ion momentum spectroscopy to a molecule, employing a time-of-flight (TOF) mass-spectrometer with a position-sensitive ion detector, where ions are produced by resonance enhanced multi-photon ionization (REMPI). We chose to study the ionization of NO molecules cooled in a supersonic nozzle beam because of the low NO ionization potential and because its ionization is well known in literature [13–20]. To our knowledge, to date there exists only one similar study, in which the recoil energy and angular distribution of ^{87}Rb ions are determined [11,12].

2. Experimental

The experiment has been described previously [21–23] except that a continuous molecular beam and a position-sensitive detector are used. The last modifications of the apparatus are given in [24–26], only a brief summary is given here. The basic experimental scheme (Fig. 1) includes a cold supersonic molecular beam, state-selective REMPI detection of photofragments, and a home-built single-field TOF mass-spectrometer combined with a position-sensitive ion detector. A one-color (1 + 1) REMPI scheme for NO preparation and probing via

* Corresponding author. Fax: +5313915396.
E-mail address: c.maul@tu-braunschweig.de (C. Maul).

0009-2614/$ - see front matter © 2004 Elsevier B.V. All rights reserved.
doi:10.1016/j.cplett.2004.04.002

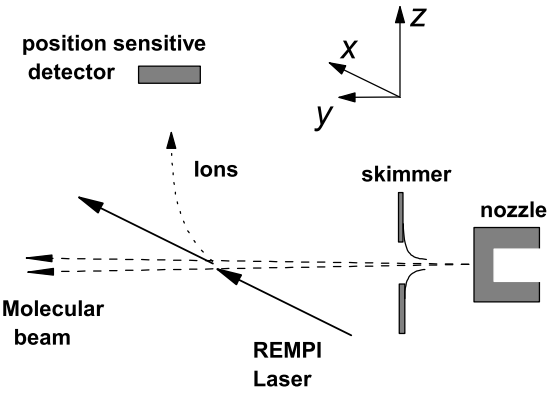

Fig. 1. Schematic depiction of REMPI/TOF mass-spectrometer with position-sensitive detector provided for 3-dimensional photofragment imaging. Also shown is the axis system used in this work.

$$\mathrm{NO}(\mathrm{X}^2\Pi_{1/2}, v=0, J) \overset{+h\nu}{\rightarrow} \mathrm{NO}(\mathrm{A}^2\Sigma^+, v^*=0, N^*) \overset{+h\nu}{\rightarrow} \mathrm{NO}^+(^1\Sigma, v^+=0, N^+) + e^-$$

around 226.2 nm is used (Fig. 2) [27]. Here, v denotes vibrational quantum numbers and N and J are rotational quantum numbers for Hund's cases b and a, respectively. A Nd:YAG-laser-pumped dye laser (Coherent Infinity/Lambda Physik Scanmate, 100 Hz) operated with Coumarin-47 dye and frequency doubling in a BBO crystal is used.

The vacuum system consists of jet and ionization chambers separated by a skimmer with 0.4 mm diameter. A cold continuous molecular beam is obtained by supersonic expansion of a gas mixture NO/Ar ($1{:}10^5$) at six bar pressure through a 20 μm nozzle. The molecular beam speed 554 m/s and the NO rotational and translational temperatures are ≈3.5 K [24,25]. Distances nozzle–skimmer and skimmer–laser

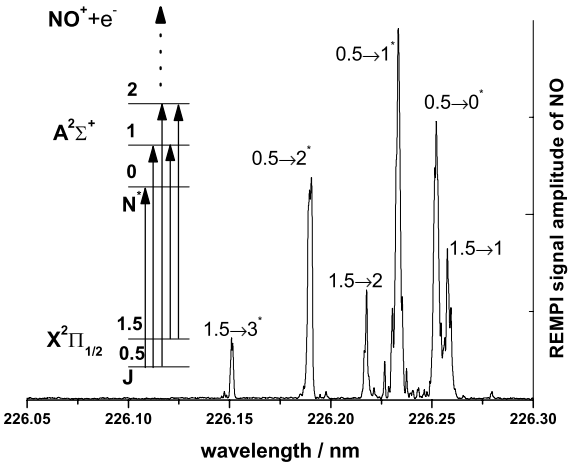

Fig. 2. Rotational (1 + 1) REMPI spectrum of NO in the cold Ar molecular beam. $J \rightarrow N^*$ assignment of the strongest rotational transitions is indicated. The transitions used in the present study are marked by asterisks.

beam are 1.5 and 30 cm, respectively. The molecular beam divergence is less than 0.1 mrad for a laser focus radius of 20 μm and geometric cooling reduces the Z component of the initial NO velocity to only 0.04 m/s. In the ionization chamber the skimmed molecular beam is intersected by the laser beam whose propagation direction (X-axis) is perpendicular to the molecular beam (Y-axis). NO^+ generated by REMPI in the ionization chamber of the spectrometer is accelerated along the Z-axis by a 2.3 V/cm electric field towards the field-free drift region. Ions are detected by a 8 cm diameter double stage multi-channel plate assembly and a position-sensitive detector (Roentdek). Only TOF profiles are analyzed in the present study. The laser power was kept low, typically in the range 6–15 μJ, to avoid saturation effects, corresponding to peak intensities of $(2\text{–}5) \times 10^8$ W/cm^2 in the laser focus. About one NO^+ photo ion was registered per 10 laser shots. Typically about 40 000 laser shots were accumulated for each TOF distribution.

Our detector was developed by Jagutzki et al. [30] and consists of a delay-line anode introduced into the ionization chamber right behind the multi-channel plate [28,29]. We used a similar electronic read-out circuit as described in [31]. Detector resolution is 0.4 mm in space (1:200) and about 0.5 ns in time [24,25].

An additional potential (≈300 V) applied between multi-channel plate and detector accelerates the electrons to the delay-line anode where a signal is induced which propagates in both directions towards the ends of the line where impedance adjusted circuits pick it up for further processing. By measuring the time period between the signal arrival times on both ends of the line one can determine the position of the signal source on the line. The detector consists of two individual delay lines oriented orthogonal to each other, forming the XY plane (8×8 cm). The output charge from the multi-channel plate resulting from every single incoming ion or photon ('event') produces altogether four signals, two on each delay line pair which are transmitted to time-to-digital converters. Finally, one event produces two pairs of times, X_1, X_2 and Y_1, Y_2. X and Y coordinates of a single event in time units are calculated as $(X_1 - X_2,\ Y_1 - Y_2)$, and the event time (the Z coordinate) is calculated as either $(X_1 + X_2)/2$ or $(Y_1 + Y_2)/2$. Thus the delay-line detector yields all three coordinates of each single event. The latter condition allows to distinguish between true and false events: the event time provided by the different delay lines must coincide: $(X_1 + X_2)/2 = (Y_1 + Y_2)/2$. Only events that obey this condition are taken into account, and all others are ignored. If more than one ion per laser pulse strikes the multi-channel plate assembly, each delay line produces a series of pulses and the criterion $X_1 + X_2 = Y_1 + Y_2$ allows to correctly assign individual pulses to individual ions.

3. Results and discussion

3.1. TOF profiles

Fig. 3 shows typical TOF spectra of NO^+ ions recorded in experiments with different laser polarizations, $E \perp Z$ and $E \| Z$, where E is the electric field of the laser radiation. A clearly resolved double-peaked structure in the $E \| Z$ TOF spectrum is due to preferential emission of the NO^+ along the laser polarization. The theoretical angular distribution of NO^+ ions detected by $(1+1)$ REMPI is [12,14,16]

$$I(\theta) = \frac{1}{4\pi}[1 + \beta_2 P_2(\cos\theta) + \beta_4 P_4(\cos\theta)], \tag{1}$$

P_2 and P_4 are Legendre polynomials ($P_2(x) = [3x^2 - 1]/2$, $P_4(x) = [35x^4 - 30x^2 + 3]/8$), θ is the polar spherical angle, and β_2 and β_4 are anisotropy parameters.

The axis of the spherical coordinate system is directed along the electric field of the laser radiation. For a given speed v_0, using Eq. (1) we can find expressions for TOF distributions as

$$\begin{aligned} H_{x,z}(t) &= a_{x,z} + b_{x,z}[(t-t_0)/\Delta t]^2 \\ &\quad + c_{x,z}[(t-t_0)/\Delta t]^4, && \text{if } |t-t_0| \leqslant \Delta t, \\ &= 0, && \text{if } |t-t_0| > \Delta t, \end{aligned} \tag{2}$$

where the coefficients are

$$\begin{aligned} a_z &= 1/2 - \beta_2/4 + 3\beta_4/16, & a_x &= 1/2 + \beta_2/8 + 9\beta_4/128, \\ b_z &= 3(2\beta_2 - 5\beta_4)/8, & b_x &= -3\beta_2/8 - 45\beta_4/64, \\ c_z &= 35\beta_4/16, & c_x &= 105\beta_4/128, \end{aligned}$$

where t and t_0 are the individual and average TOF, respectively; the indices x and z correspond to $E \perp Z$ and $E \| Z$ laser polarizations, respectively; the distributions are normalized to unity, $(1/\Delta t)\int_{-\infty}^{\infty} H_{x,z}(t)\mathrm{d}t = 1$. The time Δt may be calculated as

$$\Delta t = v_0/A, \tag{3}$$

where A is the acceleration of the NO^+ ions due to external electric field E_{ex}, $A = eE_{ex}/M_{NO}$. Ions with the initial speeds v_0 and $-v_0$ along Z-axis have the TOFs of $t_0 - \Delta t$ and $t_0 + \Delta t$, respectively. The initial recoil speed of the ions is

$$v_0 = m_e/M_{NO}\sqrt{2(2h\nu - I_{NO})/m_e}, \tag{4}$$

where m_e and M_{NO} are the masses of the electron and of NO, respectively, $h\nu$ is the 226 nm photon energy, and $I_{NO} = 9.2639$ eV is the first NO ionization potential. From Eq. (4) we find $v_0 = 14.1$ m/s. With the experimental values of $t_0 = 22.78$ μs and $E_{ex} = 2.3$ V/cm, we obtain $\Delta t = 19.1$ ns. The recoil energy of NO^+ is $M_{NO}v_0^2/2 = 31.2$ μeV. This is much larger than the kinetic energy of the jet-cooled NO parent molecules in the Z-direction which is less than 1 neV due to geometric cooling.

3.2. Broadening of TOF profiles

Eq. (2) predicts sharp corners of the TOF distribution at $t = t_0 \pm \Delta t$. One can see from Fig. 3 that the experimental TOF profiles do not have sharp corners and that they spread outside $|t - t_0| > \Delta t$ time range. Hence additional broadening mechanisms need to be considered. Assuming that the broadened TOF profile may be derived from convoluting expression (2) with a Gaussian distribution, one obtains

$$G_{x,z}(t) = \int_{-\infty}^{\infty} \exp\left(-\left[\frac{t-q}{\delta\Delta t}\right]^2\right) H_{x,z}(q)\,\mathrm{d}q, \tag{5}$$

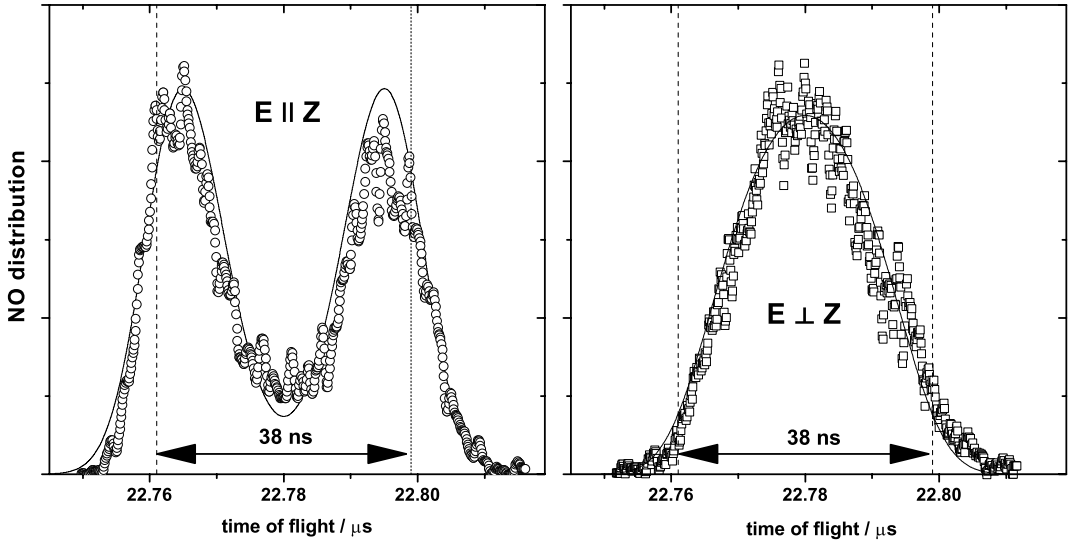

Fig. 3. Time-of-flight profiles of NO detected by $(1+1)$ REMPI at 226 nm at different polarizations, TOF = 22.78 μs and $N^* = 1$. The range of times $t_0 \pm \Delta t$ is shown by two dashed lines. The curves are calculated with Eq. (6).

where the dimensionless parameter δ characterizes the profile broadening. The same assumption was done by Wolf and Helm [12]. Integration of expression Eq. (5) yields

$$G_{x,z}(t) = [F_{x,z}(t) - F_{x,z}(-t)]/G_0, \tag{6}$$

where

$$F_{x,z}(t) = \frac{\delta^2}{4} e^{-\frac{\tau^2+2\tau+1}{\delta^2}} \left[2c\tau^3 - 2c\tau^2 + \tau(2b + 5\delta^2 c + 2c) - 2b - 3\delta^2 c - 2c\right] + \frac{\sqrt{\pi}\delta}{8} \operatorname{erf}^{\frac{\tau+1}{\delta}} \left[4c\tau^4 + 4\tau^2(b + 3\delta^2 c) + 4a + 2b\delta^2 + 3\delta^4 c\right],$$

$$G_0 = \frac{2\sqrt{\pi}|\delta|[15a + 5b + 3c]}{15}, \tag{7}$$

where $\tau \equiv (t - t_0)/\Delta t$. For the sake of brevity the x, z indices of the a, b, c, and G_0 parameters are omitted. The factor G_0 normalizes the function $G_{x,z}$ to unity: $(1/\Delta t) \int G_{x,z}(t)\, dt = 1$. The experimental TOF profiles for both polarizations were fitted by Eq. (6) with the fit parameters β_2, β_4, δ, and Δt. Accurate fitting of the best experimental TOF profiles showed that the fitted Δt parameters are very close to the value calculated with Eq. (3); hence we used only the calculated value. The broadening parameter δ was found to be 0.32 ± 0.05.

One can propose several broadening mechanisms. One is the duration of the laser pulse. According to Eq. (5), the ions which start from the same space point with equal initial speeds produce the TOF distribution with a FWHM (full width at half maximum) of 10.2 ns, this broadening is much larger than the duration of the laser pulse (~3 ns). Hence, the duration of the laser pulse cannot explain the observed broadening.

Broadening due to electric field inhomogeneity may be neglected because different parts of the image of the NO molecular beam on the delay-line detector (6×3 mm) give the same TOF distribution.

In our spectrometer the acceleration length L_1 is half as long as the drift length L_2, $2L_1 = L_2$. For slow particles this constitutes a spatial focusing configuration; i.e., $t_0 = (2L_1 + L_2)/\sqrt{2AL_1}$ and $dt_0/dL_1 = 0$. Thus, the effect of the finite size of the focal volume is also negligible.

The NO speed distribution along the Z-axis has a maximum velocity of ~4 cm/s. This speed is negligible in comparison with v_0, hence the thermal contribution may be neglected.

We did observe a correlation between laser power and the broadening parameter δ, thus space–charge effects are the most probable reasons for broadening, i.e., the interaction between NO^+ and other ions produced by the same laser pulse from background gas.

Neglecting laser pulse duration, we predict from Eq. (6) that ions with the same starting coordinates and initial velocities produce a speed distribution with a FWHM of 7.5 m/s due to space charge effects, corresponding to 9 μeV (104 mK), characterizing the energy resolution of our method. In the Rb atom study of Wolf and Helm [11,12] using a magneto-optical trap the energy resolution was much better, about 0.2 μeV (2.3 mK). Their background pressure was only 4×10^{-9} mbar, while in our experiments it was $\sim 2 \times 10^{-7}$ mbar. Very probably, the resolution of our method may be improved by better pumping or change of background gases in order to minimize the non-resonant generation of ions.

3.3. β_2 and β_4 parameters

β_2 and β_4 parameters obtained from the fits for $N^* = 0, 1, 2, 3$ are summarized in Table 1. The β_4 parameter for $N^* = 0$ must be zero, since the rotational state is isotropic; the non-zero β_4 parameter in Table 1 may be due to a small contribution of the transition via $N^* = 1$ (see Fig. 1).

From Table 1 one can see rather large variations in our β_2 and β_4 values. A correlation of these values with the intensity of the laser radiation exists, but is insignificant within the experimental error. Note that the

Table 1
Summary of the data on on β_2 and β_4 parameters in the (1 + 1) REMPI of NO via $(X^2\Pi_{1/2}, v = 0, J) \rightarrow (A^2\Sigma^+, v^* = 0, N) \rightarrow ({}^1\Sigma, v^+ = 0, N^+)$

Transition	$J \rightarrow N$	Experiment		Calculation		References
		β_2	β_4	β_2	β_4	
$Q_{11} + P_{21}(0.5)$	$0.5 \rightarrow 0$	1.75(0.05)	0.15(0.15)			[a]
$Q_{21} + R_{11}(0.5)$	$0.5 \rightarrow 1$	1.90(0.07)	0.6(0.2)			[a]
$R_{21}(0.5)$	$0.5 \rightarrow 2$	1.40(0.10)	0.0(0.1)			[a]
$R_{21}(1.5)$	$1.5 \rightarrow 3$	1.35(0.10)	0.1(0.1)			[a]
$Q_{21} + R_{11}(21.5)$	$21.5 \rightarrow 22$			1.628[b]	−0.386[b]	[14]
$R_{21}(20.5)$	$20.5 \rightarrow 22$	1.534	0.270	1.346	−0.0485	[15]
$Q_{11} + P_{21}(25.5)$	$25.5 \rightarrow 25$	1.589	0.024	1.602	−0.0387	[15]
$Q_{11} + P_{21}(22.5)$[c]	$22.5 \rightarrow 22$	1.573	−0.0175	1.578	−0.093	[16]
$Q_{11} + P_{21}(2.5)$	$2.5 \rightarrow 2$			1.576	−0.1002	[17]

[a] This work. The value in parenthesis represents 1σ uncertainty.
[b] For $\Delta N = 0$ branch only.
[c] Vibrational states: $v = 0$, $v^* = 1$, and $v^+ = 1$.

depolarization of the NO in the intermediate state $A^2\Sigma^+$ cannot explain these variations since depolarization occurs at times much larger than the laser pulse duration [18,19].

The anisotropy parameters β_2 and β_4 have previously been determined for large J values by REMPI-PES [15]. For the J values considered, the energy resolution of this method allowed to determine state-specific anisotropy parameters depending on the rotational state of the molecular ion. The weighted averages of the published anisotropy parameters obtained in these measurements are also listed in Table 1 and compare favorably to the data obtained from our recoil ion measurements for low values of J. Due to the smallness of the momentum transferred onto the molecular ion by ejection of a photoelectron, rotational resolution of the states of the molecular ion cannot be achieved in our measurements.

4. Summary

We observed for the first time the ion recoil from the ionization of a molecule by REMPI/TOF. We demonstrated that the technique is applicable to study the velocity (speed and angle) distributions of ions obtained from the recoil in photoionization. The main advantages of the technique are its relative simplicity and versatility. The resolution of the method of about 10 μeV can significantly be improved if space–charge effects are avoided. The merit of the method lies mainly in investigating complex ionization processes involving fragmentation of the neutral molecule or the molecular ion which cannot be studied by photoelectron spectroscopy alone.

Acknowledgements

This work was supported by the Deutsche Forschungsgemeinschaft. A.I. Chichinin gratefully thanks the Alexander von Humboldt Foundation for support. T.S. Einfeld acknowledges support of the Fonds der Chemischen Industrie.

References

[1] R. Dörner, J. Ullrich, H. Schmidt-Böcking, R.E. Olson, Phys. Rev. Lett. 63 (1989) 147.
[2] V. Frohne, S. Cheng, R. Ali, M. Raphaelian, C.L. Cocke, R.E. Olson, Phys. Rev. Lett. 71 (1993) 696.
[3] C.R. Monroe, E.A. Cornell, C.A. Sackett, C.J. Myatt, C.E. Wieman, Phys. Rev. Lett. 70 (1993) 414.
[4] R. Dörner, V. Mergel, R. Ali, U. Buck, C.L. Cocke, K. Froschauer, O. Jagutzki, S. Lencinas, W.E. Meyerhof, S. Nuttgens, R.E. Olson, H. Schmidt-Böcking, L. Spielberger, K. Tokesi, J. Ullrich, M. Unverzagt, W. Wu, Phys. Rev. Lett. 72 (1994) 3166.
[5] R. Moshammer, J. Ullrich, M. Unverzagt, W. Schmidt, P. Jardin, R.E. Olson, R. Mann, R. Dörner, V. Mergel, U. Buck, H. Schmidt-Böcking, Phys. Rev. Lett. 73 (1994) 3371.
[6] V. Mergel, R. Dörner, J. Ullrich, O. Jagutzki, S. Lencinas, S. Nuttgens, L. Spielberger, M. Unverzagt, C.L. Cocke, R.E. Olson, M. Schulz, U. Buck, E. Zanger, W. Theisinger, M. Isser, S. Geis, H. Schmidt-Böcking, Phys. Rev. Lett. 74 (1995) 2200.
[7] J. Ullrich, R. Moshammer, R. Dörner, O. Jagutzki, V. Mergel, H. Schmidt-Böcking, L. Spielberger, J. Phys. B 30 (1997) 2917.
[8] R. Moshammer, B. Feuerstein, W. Schmitt, A. Dorn, C.D. Schröter, J. Ullrich, H. Rottke, C. Trump, M. Wittmann, G. Korn, K. Hoffmann, W. Sandner, Phys. Rev. Lett. 84 (2000) 447.
[9] A. Lafosse, M. Lebech, J.C. Brenot, P.M. Guyon, O. Jagutzki, L. Spielberger, M. Vervloet, J.C. Houver, D. Dowek, Phys. Rev. Lett. 84 (2000) 5987.
[10] Th. Weber, M. Weckenbrock, A. Staudte, L. Spielberger, O. Jagutzki, V. Mergel, F. Afaneh, G. Urbasch, M. Vollmer, H. Giessen, R. Dörner, Phys. Rev. Lett. 84 (2000) 443.
[11] S. Wolf, H. Helm, Phys. Rev. A 56 (1997) R4385.
[12] S. Wolf, H. Helm, Phys. Rev. A 62 (2000) 43408.
[13] W.G. Wilson, K.S. Viswanathan, E. Sekreta, J.P. Reilly, J. Phys. Chem. 88 (1984) 672.
[14] S.N. Dixit, D.L. Lynch, V. McKoy, W.M. Huo, Phys. Rev. A 32 (1985) 1267.
[15] S.W. Allendorf, D.J. Leahy, D.C. Jacobs, R.N. Zare, J. Chem. Phys. 91 (1989) 2216.
[16] D.J. Leahy, K.L. Reid, R.N. Zare, J. Chem. Phys. 95 (1991) 1757.
[17] K.L. Reid, D.L. Leavy, R.N. Zare, J. Chem. Phys. 95 (1991) 1746.
[18] K.L. Reid, Chem. Phys. Lett. 215 (1993) 25.
[19] K.L. Reid, S.P. Duxon, M. Towrie, Chem. Phys. Lett. 228 (1994) 351.
[20] S.C. Althorpe, T. Seideman, J. Chem. Phys. 110 (1999) 147.
[21] C. Maul, T. Haas, K.-H. Gericke, F.J. Comes, J. Chem. Phys. 102 (1995) 3238.
[22] C. Maul, T. Haas, K.-H. Gericke, J. Phys. Chem. A 101 (1997) 6619.
[23] M. Roth, C. Maul, K.-H. Gericke, T. Senga, M. Kawasaki, Chem. Phys. Lett. 305 (1999) 319.
[24] A.I. Chichinin, T.S. Einfeld, K.-H. Gericke, C. Maul, in: B. Whitaker (Ed.), Imaging in Molecular Dynamics: Technology and Applications, Cambridge University Press, Cambridge, 2003, p. 138.
[25] A.I. Chichinin, T.S. Einfeld, C. Maul, K.-H. Gericke, Rev. Sci. Instrum. 73 (2002) 1856.
[26] T.S. Einfeld, A.I. Chichinin, C. Maul, K.-H. Gericke, J. Chem. Phys. 116 (2002) 2803.
[27] J. Danielak, U. Domin, R. Kepa, M. Rytel, M. Zachwieja, J. Mol. Spectrosc. 181 (1997) 394.
[28] M. Lampton, O. Siegmund, R. Raffanti, Rev. Sci. Instrum. 58 (1987) 2298.
[29] S.E. Sobottka, M.B. Williams, IEEE Trans. Nuc. Sci. 35 (1988) 348.
[30] O. Jagutzki, V. Mergel, K. Ullmann-Pfleger, L. Spielberger, U. Meyer, H. Schmidt-Böcking, Proc. SPIE 19.7–24.7 (1998).
[31] M. Brown, M. Beckert, U. Müller, Rev. Sci. Instrum. 71 (2000) 4535.